RSC Advances

ROYAL SOCIETY OF CHEMISTRY

www.rsc.org/advances

Bromate Reduction in Water by Catalytic Hydrogenation using Metal Organic Frameworks and Sodium Borohydride

*Kun-Yi Andrew Lin** *and Shen-Yi Chen*

Department of Environmental Engineering, National Chung Hsing University,

250 Kuo-Kuang Road, Taichung, Taiwan, R.O.C.

*Corresponding Author. Tel: +886-4-22854709, E-mail address: linky@nchu.edu.tw

(Kun-Yi Andrew Lin)

Abstract

Catalytic hydrogenation of bromate is a promising approach to remove bromate from water considering that this approach not only removes bromate but also converts it to bromide. However, the reduction of metal catalysts and the bromate reduction using continuous H_2 purge inevitably lead to waste of H_2 gas. Thus, using solid H_2-releasing compounds (*e.g.*, $NaBH_4$) to generate H_2 *in-situ* seems to be more advantageous because solid H_2-releasing compounds are relatively safe and easy to handle. Recently, Metal Organic Frameworks (MOFs) has attracted enormous attention owing to its superior physical and chemical characteristics in CO_2 capture and H_2 storage. Some non-noble-metal MOFs also have been extensively used as catalysts, including hydrolysis of $NaBH_4$ for H_2 production. Nevertheless, few studies have studied of using MOFs as heterogeneous catalysts to produce hydrogen *in-situ* and then reduce bromate. In fact, metallic catalysts coupled with $NaBH_4$ have not been evaluated for the bromate reduction. Thus, this study aims to investigate whether MOFs/$NaBH_4$ can be an effective system to reduce bromate. The iron-bearing MOF, MIL-88A, and the cobalt-bearing MOF, ZIF-67, were selected owing to their non-noble metallic contents. While $NaBH_4$ alone was found to reduce bromate, the combination of MOFs/$NaBH_4$ considerably accelerated the hydrolysis of $NaBH_4$, thereby reducing bromate to bromide. The effect of $NaBH_4$ dosage was found to be the most influential on the removal efficiency and kinetics, while the effect of MOF loading was insignificant. Elevated temperatures and relatively acidic conditions were also more favorable for the bromate reduction. In the presence of other anions, MOFs/$NaBH_4$ still successfully reduced bromate to bromide. MOFs/$NaBH_4$ can be also re-used for the bromate reduction and ZIF-67/$NaBH_4$ even exhibited almost 100% of recyclability after 5 cycles. The above-mentioned results indicate that MOFs can

successfully facilitate the hydrolysis of $NaBH_4$ and subsequently reduce bromate to bromide in water.

Keywords: MOFs, ZIF-67, MIL-88A, Bromate, Sodium Borohydride

1. Introduction

Ozonation of bromide in water leads to formation of hypobromous acid and hypobromite, which can be further oxidized to bromate (BrO_3^-) by ozone/radicals. Bromate has been classified as a 2B substance according to the International Agency for Research on Cancer (IARC) [1], and the United States Environmental Protection Agency and the World Health Organization regulate its maximal contaminant level to 10 μg L^{-1} in drinking water, considering its potential carcinogenicity [1]. As ozonation process is increasingly used as a secondary water treatment [2] , there is an urge need to develop effective processes to remove bromate from water.

Typically bromate contamination can be eliminated from water via the following strategies: removal of bromate precursors, prevention of bromate formation during ozonation and removal of bromate from water after it is formed. Although removal of bromate precursors should be the most ideal strategy, it is difficult to remove bromate precursors efficiently in conventional wastewater treatments[3]. On the other hand, complete prevention of the bromate formation is extremely challenging and current attempts to minimize the bromate formation slow disinfection process and generate ammonia [4]. Therefore, the direct removal of ozonation-derived bromate from water appears to be a more feasible approach.

A number of methods have been proposed to remove bromate from water, such as filtration [5], adsorption [6] and ion exchange [7]. Even though these methods can remove bromate from water, aqueous bromate contamination is transferred to solid forms of bromate pollution (*i.e.*, bromate on membranes, filters, adsorbents and ion exchange resins) or highly concentrated bromate solutions. The toxicity of bromate still remains and it has to be additionally treated. Considering this issue, the catalytic hydrogenation of bromate is more advantageous because it not only removes bromate

from water but also reduces bromate to bromide which is significantly less concerning. Up to date, a few studies have demonstrated the bromate reduction using the catalytic hydrogenation. Chen *et al.* used alumina-supported palladium (Pd/Al_2O_3) as a catalyst with purge of hydrogen (H_2) gas to reduce bromate to bromide [8] in water. Marco *et al.* developed carbon nanofiber-supported ruthenium and palladium (*i.e.*, Ru-CNF and Pd-CNF) with H_2 purge to reduce bromate [9]. Restivo *et al.* also evaluated different transition metals supported on activated carbon, including palladium, platinum, iridium, rhodium, ruthenium, iron, tin, copper, zinc and nickel, with H_2 purge to reduce bromate [10]. To facilitate recovery of catalysts from solutions, Sun *et al*. also prepared a palladium-based magnetic catalyst (Pd/Fe_3O_4) with H_2 purge to reduce bromate [11]. The hydrogenation of bromate could be also achieved in another means by using zerovalent metals which were first reduced using H_2-based reducing agents and then used to reduce bromate [12]. In fact, the above-mentioned transition metals were also reduced using H_2; the reduced transition metals were then combined with H_2 gas to convert bromate to bromide.

Apart from that these metallic catalysts have to be reduced by H_2 purge, the bromate reduction reaction also involved the continuous H_2 purge to increase availability of H_2 in order to improve the reduction reaction. The continuous H_2 purge for the reduction of metallic catalysts and the bromate reduction inevitably leads to waste of H_2 gas because of the limited solubility of H_2 gas in water [13]. Additionally, when the metallic catalysts were reduced using H_2 prior to the bromate reduction, a significant amount of H_2 and preparation time is also required, especially considering that most of the metal catalysts for the hydrogenation of bromate are noble metals (*e.g.*, Pd and Ru)[10]. Moreover, pre-purged H_2 in water can still escape from reaction solutions due to stirring or shaking during the bromate reduction. Therefore, it is

necessary to develop a more-efficient, less-expensive and more-controllable method to hydrogenate bromate. As H_2, the reducing agent, has to be provided to hydrogenate bromate/reduce metals, solid H_2-releasing compounds seem to be a promising alternative to provide H_2. The solid H_2-releasing compounds, such as sodium borohydride ($NaBH_4$), recently have attracted great attention because they can release highly pure H_2 [14]. Unlike gaseous hydrogen, an advantage of these solid H_2-releasing compounds is relatively easy and safe to handle [15, 16]. Despite the fact that self-hydrolysis of $NaBH_4$ is slow, the hydrolysis process can be greatly facilitated using catalysts. This means that the release of hydrogen from NaBH4 can be controllable rather than instantly unmanageable H_2 release. Thus, the catalytic hydrolysis of $NaBH_4$ for hydrogen production has been considered a promising approach. Many catalysts are also proposed to facilitate the hydrolysis of $NaBH_4$, including cobalt [17], nickel [18], palladium [19], ruthenium [14], indium [20], tin [20], antimony [20], platinum [21]. Considering that most of these catalysts involve noble metals, using non-noble-metal heterogeneous catalysts for the hydrolysis of $NaBH_4$ should be developed.

Recently, a new class of inorganic-organic crystalline hybrid materials, called Metal Organic Frameworks (MOFs), attracts enormous attention [22]. MOFs can be prepared from various metals as “nodes” and different organic ligands as “bridges” to form 3-D dimensional networks. MOFs have been shown to exhibit many superior characteristics including large pore volume and high surface area, versatile functionalities, high chemical resistance, etc.[23] These properties enable MOFs attractive materials for catalysis [24, 25] and gas adsorption/storage [26-28]. A number of non-noble-metal MOFs have been also prepared and used in various applications. The non-noble-metal MOFs include iron [29], cobalt [30], copper [31] and zinc [32] MOFs. These

MOFs have also been used as heterogeneous catalyst for the degradation of organic pollutants or the reduction of toxic metallic pollutants. For instance, the zinc-based (MOF-5) and iron-based MOFs (MIL-100) had been employed as photo-catalysts to degrade phenols and dyes under UV and visible light irradiation [33]. The zirconium-based MOFs (UiO-66) was also employed to photo-catalytically reduce toxic Cr^{6+} to Cr^{3+} in water [34]. Lately, a MOF (*i.e.*, ZIF-9) has been also evaluated as a catalyst to facilitate the hydrolysis $NaBH_4$ and the result shows that MOFs can greatly facilitate the hydrogen production via the hydrolysis of $NaBH_4$ [35].

While MOFs have been proven as effective and promising heterogeneous catalysts in many reactions including the hydrolysis of $NaBH_4$, few studies have studied of using MOFs as heterogeneous catalysts to produce hydrogen *in-situ* and then reduce bromate via the hydrogenation. In fact, to our best knowledge, metallic catalysts coupled with $NaBH_4$ have not been evaluated for the bromate reduction. Thus, in this study, we aim to investigate whether MOFs/$NaBH_4$ can be an effective system to reduce bromate without H_2 purge.

Although in the previous study, a cobalt-based MOF, ZIF-9, had been used to facilitate the hydrolysis of $NaBH_4$, ZIF-9 has to be prepared in N,N-dimethylformamide (DMF) [35], a carcinogenic solvent according to the IARC. If MOFs, prepared in DMF, are not well activated and have not properly undergone solvent exchange, DMF can still be encapsulated inside MOFs, leading to secondary pollution. Thus, we particularly select two non-noble metal MOFs, MIL-88A (iron-based) and ZIF-67 (cobalt-based), that are prepared just in water and methanol, respectively.

The as-synthesized MOFs were characterized using scanning and transmission electronic microscopy (SEM and TEM), powder X-ray Diffraction (PXRD),

adsorption FT-IR, thermogravimetric analyzer (TGA), X-ray photoelectron spectroscopy (XPS) and N_2 sorption/desorption isotherm. Factors influencing the bromate reduction were examined, including $NaBH_4$ dosage, MOF loading, temperature, pH and co-existing anions. The reaction kinetic data at different temperatures were also analyzed to obtain the activation energy using MIL-88A and ZIF-67 with $NaBH_4$. The recyclability of MOFs for the bromate reduction was also evaluated.

2. Experimental

Reduction of bromate using MIL-88A and ZIF-67 in the presence of $NaBH_4$

In this study, MIL-88A and ZIF-67 were prepared according to the reported procedures as illustrated in Fig. 1 [30, 36], and synthesis and characterization details can be found in the supporting information. Reduction of bromate using MOFs/$NaBH_4$ was evaluated by batch-type experiments. In a typical test, a certain amount of $NaBH_4$ (*e.g.*, 250 mg) was first added to 0.5 L of bromate solution with an initial concentration (C_0 = 100 mg L^{-1}) at a constant temperature (*e.g.*, 25 °C). Once $NaBH_4$ was fully dissolved in the bromate solution (less than 1 min), a given amount of MOFs (*e.g.*, 250 mg) was subsequently added to the bromate solution. Sample aliquots were withdrawn from the resultant mixture at pre-set times. Remaining concentration (C_t) of bromate and resulting bromide (Br^-) of aliquots were determined using an ion chromatography system (Dionex ICS-1100 Basic Integrated IC System, USA). To investigate the effect of the reducing reagent, $NaBH_4$ dosage was varied from 0 to 1000 mg L^{-1}, whereas concentration of MIL-88A (or ZIF-67) changed from 250 to 1000 mg L^{-1} to examine the effect of MOF loading. The solution temperature

was also changed from 25 to 75 °C to examine the effect of temperature and to determine the corresponding rate constants (k) and activation energy (E_a).

In this study, the main goal is not just to remove bromate from water but also to convert bromate to bromide via the reductive reaction. To directly evaluate amounts of bromate removal and conversion, the removal efficiency (q_t) was intentionally expressed by mmol of bromate (or bromide) per gram of MOFs (*i.e.*, mmol g^{-1}) as follows (Eq.1):

$$q_t = \frac{V|C_0 - C_t|}{W} \qquad (1)$$

where W (g) is the amount of MOFs added in the reduction experiment; V (L) is the total volume of solution; C_t (mmol L^{-1}) represents the molar concentration (mmol L^{-1}) of bromate (or bromide) at a given time, t (min), whereas C_0 (mmol L^{-1}) is the initial molar concentration of bromate (or bromide). For investigating effects of pH and co-existing anions, and recyclability of MOFs for the bromate reduction, experimental details can be found in the supporting information.

3. Results and Discussion

3.1 Characterization of the as-synthesized MIL-88A and ZIF-67

Morphology of the as-synthesized MIL-88A can be found in Fig. 2(a), in which MIL-88A nanorods are closely-packed after the preparation process. The hexagonal shape of MIL-88A nanorods are still easily recognized as the reported MIL-88A [37, 38]. The aggregated MIL-88A nanorods can be mono-dispersed in solvents (*e.g.*, water) assisted by sonication. A TEM image (Fig. S1(a), see ESI†) shows a single MIL-88A nanorod which is about 600 nm-long; the size distribution of MIL-88A nanorods is also summarized in Fig. S1(b). The length of MIL-88A nanorods ranges from 100 to

800 nm with an average length of 300 nm. Crystalline structure of MIL-88A was further analyzed and shown in Fig. 2(b). It has been revealed that synthesis parameters, such as temperature, pressure, solvent selection and pH, greatly affect the PXRD pattern of MIL-88A [37, 39]. Since MIL-88A in this study was synthesized in water at 85 °C under ambient pressure, the XRD pattern agrees with the reported XRD pattern of MIL-88A which was synthesized under similar conditions [37]. We also measured the IR spectrum of MIL-88A as shown in Fig. S2(a). Considering that MIL-88A was synthesized using fumaric acid, a number of significant bands are derived from fumaric acid. The bands at 1396 and 1603 cm^{-1} are from the symmetric and asymmetric vibration modes of the carboxyl group, respectively [40]. The band at 648 cm^{-1} is attributed to the carbonyl group [41]. Although MIL-88A was dried in the oven to remove the synthesis solvent (*i.e.*, water), the IR spectrum of MIL-88A still exhibits a broad band in the region between 3200−3400 cm^{-1} owing to the presence of water and a short band at 3572 cm^{-1}, ascribed to the vibrational mode of OH^-. The water content might be from the adsorption of moisture in air to MIL-88A. The moisture content in MIL-88A is also revealed by the TG analysis. Fig. S2(b) shows the TG curve of MIL-88A and the corresponding derivative TG as the inset. A minor weight loss occurred below 100 °C, which could be attributed to the moisture and other gas molecules adsorbed to MIL-88A. However, the weight of MIL-88A remained quite stable up to 200 °C, when the ligand (*i.e.*, fumaric acid) started decomposing through 400 °C [42]. Subsequently, the weight of MIL-88A was almost unchanged through 800 °C.

To further identify the chemical composition of MIL-88A, XPS analysis was employed and the result is displayed in Fig. S3, showing a full survey of MIL-88A. Several significant peaks are readily recognized at binding energies of 284.4, 531.2,

711.4 and 725.2 eV, corresponding to C 1s, O 1s, Fe $2p_{3/2}$, and Fe $2p_{1/2}$, respectively. Fig. 2(c) shows the Fe 2p core-level spectrum of MIL-88A, in which Fe $2p_{1/2}$ and Fe $2p_{3/2}$ peaked can be clearly revealed. The peak separation between Fe $2p_{1/2}$ and Fe $2p_{3/2}$ is also determined and found to be ~13.8 eV, which is comparable to the value reported for Fe_2O_3. This indicates that iron existing within MIL-88A coordinated with oxygen of fumaric acid to form iron oxide clusters in the form of Fe_2O_3 [38, 43]. N_2 sorption and desorption of MIL-88A was also measured and shown in Fig. S4. The N_2 sorption isotherm of MIL-88A can be considered a combination of the type II and III isotherms, suggesting that MIL-88A might exhibit macropores as seen in the inset of Fig. S4. Its surface area and total pore volume were found to be 22 m^2 g^{-1} and 0.095 cm^3 g^{-1}, respectively. Such low surface area and pore volume can be due to that the structure of MIL-88A is flexible and the pores of MIL-88A might be closed during the degassing process of N_2 sorption and desorption measurement [44].

As for the characterization of ZIF-67, its morphology of ZIF-67 can be seen in Fig. 3(a), showing a number of ZIF-67 particulates closely-packed and aggregated after the drying treatment. The mono-dispersed ZIF-67 particulates can be seen in a TEM image (Fig. S5(a)), in which chamfered cubic shape (also called truncated rhombic dodecahedron) of ZIF-67 can be observed. It has been reported that the morphology of ZIF could be changed using different molar ratios of the metal ion amount over the ligand, as well as the synthesis duration [45]. A relatively high molar ratio (*e.g.*, 1/2) could produce rhombic-dodecahedral ZIFs which consist of 2-MIM as the ligand. When a relatively low ratio of the metal ion over the ligand (*e.g.*, 1/4 or lower) is adopted, the morphology of ZIF can become to the chamfered cube. Because the molar ratio employed in this study was 1/4, it was expected to result in the chamfered-cubic ZIF. Thus, the chamfered cube observed in Fig. 3(a) and Fig. S5(a)

indicates that ZIF-67 was well-developed during the synthesis. The size distribution of ZIF-67 nanoparticles can be also found in Fig. S5(b), ranging from 200 from 600 nm. Although the formation of zeolitic imidazole frameworks (ZIFs) resulted from the chemical bonding between metal ions and organic ligands, the selection of salts for metal ions can also directly alter the size of ZIFs [30]. Since the cobalt metal ion used in this study was from cobalt nitrate, the resultant ZIF was expected to be the middle-size ZIF (*i.e.*, < 1000 nm), which is in accordance with the observational size of ZIF-67 in Fig. 3(a).

To confirm the crystalline structure of the as-synthesized ZIF-67, XRD pattern of ZIF-67 was measured and shown in Fig. 3(b). The pattern could be readily indexed according to the reported and simulated pattern of ZIF-67 [46]. The XRD result validates that ZIF-67 was successfully synthesized and well developed.

The as-synthesized ZIF-67 was also analyzed using the adsorption FT-IR to investigate its surface chemistry. The IR spectrum of ZIF-67 is displayed in Fig. S6(a), in which the peaks were primarily derived from the ligand, 2-MIM. Positions of these peaks are consistent with the reported spectrum of ZIF-67 [46-48]. In particular, the peaks in the range of 600–1500 cm^{-1} could be assigned to the stretching and bending modes of the imidazole ring. The peak at 1584 cm^{-1} is derived from the stretching mode of C=N bonding in 2-MIM. The peaks at 2929 and 3135 cm^{-1} could be attributed to the stretching mode of C-H from the aromatic ring and the aliphatic chain in 2-MIM, respectively. Fig. S6(b) shows the thermogravimetric (TG) curve and the derivative TG curve of ZIF-67 (the inset). One can see that ZIF-67 first lost the weight from 100 to 200 °C due to the escape of guest molecules (*e.g.*, methanol or 2-MIM) as well as gas molecules from its cavities [49]. Subsequently, a major weight

loss of ZIF-67 occurred in the range of 250−500 °C, which could be attributed to the decomposition of the ligand [49].

The chemical composition of ZIF-67 was further determined using XPS. Fig. S7 reveals a full survey of ZIF-67. Several significant peaks are readily recognized at binding energies of 284.4, 399.3, 531.2, 780.6 and 796.1 eV, corresponding to C 1s, N 1s, O 1s, Co $2p_{3/2}$, and Co $2p_{1/2}$, respectively. Fig. 3(c) shows the Co 2p core-level spectrum of ZIF-67 which is deconvoluted to display peaks of cobalt species. It has been reported that peaks at 780.2 ± 0.6 and 781.8 ± 0.6 eV can be assigned to Co^{3+} and Co^{2+} ions [50, 51], respectively. Relatively small peaks at 786.3 and 804.8 eV are considered as the shake-up satellite peaks of CO^{2+} [51].

Additionally, ZIF-67 was analyzed using N_2 sorption and desorption (Fig. S8) to determine its surface and porosity. The N_2 sorption isotherm of ZIF-67 appears to be a combination of the type I and II isotherms, indicating that ZIF-67 might possess microporous and macroporous pores as revealed in the insets of Fig. S8. The surface area is found to be 1717 $m^2 g^{-1}$ with a pore volume of 0.70 $cm^3 g^{-1}$, which is similar to the reported value of ZIF-67 [52].

3.2 Bromate Reduction in Water using MOFs/$NaBH_4$

Prior to investigating the bromate reduction using MOFs/$NaBH_4$ system, it is critical to examine whether MOFs alone can reduce bromate in water. When MOFs were added to the bromate solution, the removal of bromate might be achieved via adsorption to surface of MOFs or hydrogenation from water hydrolysis caused by MOFs. We first examined the bromate removal using MIL-88A alone. Fig. 4(a) shows that the removal efficiency (q_t) both in mg g^{-1} and mmol g^{-1} remains almost zero even after 60 min. MIL-88A did not adsorb bromate and induce water hydrolysis

for hydrogenation of bromate. The similar result is observed when ZIF-67 was present in the bromate solution, showing that MOFs alone was incapable of reducing bromate in water. On the other hand, when $NaBH_4$ alone was added to the bromate solution, the removal efficiency remained almost zero initially. However, a noticeable amount of q_t (~0.055 mmol g^{-1}) could be observed in the end of the 60-min reaction. This demonstrates that a small portion of $NaBH_4$ was self-hydrolyzed to generate hydrogen which reduced bromate. Nevertheless, the evolution of hydrogen from $NaBH_4$ alone was extremely slow and thus catalysts are required to accelerate the evolution [15]. Once MIL-88A was combined with $NaBH_4$, a significant amount of q_t (~0.25 mmol g^{-1}) was observed, even though the reaction proceeded only for 1 min. As the reaction time progressed, the q_t was found to increase and to reach equilibrium. Simultaneously, we also observed the appearance of bromide during the bromate reduction (Fig. 4(b)). By comparing the bromate removal and the resulting bromide in mmol g^{-1}, the amount of bromate removal was almost completely converted to bromide. It should be also noted that the amount of bromide generated (mmol g^{-1}) was comparable to the amount of bromate removal at a given time. This reveals that when bromate was removed from water, it was instantaneously converted to bromide. In Fig. 4(a), we also observed a similar result when ZIF-67 was combined with $NaBH_4$. It can be seen that the removal efficiency for bromate increased significantly along the reaction time. At the same time, a comparable amount (in mmol g^{-1}) of bromide was also observed, showing that bromate was hydrogenated and converted to bromide using ZIF-67/$NaBH_4$. These results indicate that the combination of MIL-88A/ZIF-67 and $NaBH_4$ successfully caused the hydrogenation of bromate. When MOFs were added to a bromate solution in the presence of $NaBH_4$, several reactions might occur as illustrated in Fig. 5 [10]. First, while no significant amount of

bromate was adsorbed to MOFs, bromate might reside on the surface of MOFs temporarily as shown in Fig. 5(a). Second, H_2 generation from the hydrolysis of $NaBH_4$ was facilitated by metal sites of MOFs. The H_2 generation from the hydrolysis of $NaBH_4$ further reacted with bromate molecular residing on the surface of MOFs to become bromide according to the following equation (Eq. 2) (Fig. 5(b)):

$$BrO_3^- + 3H_2 \rightarrow Br^- + 3H_2O \qquad (2)$$

Third, the H_2 generation from the hydrolysis of $NaBH_4$ could also react with bromate in the bulk phase to become bromide as Fig. 5(c). Fourth, as revealed in the afore-mentioned XPS results, MIL-88A and ZIF-67 both comprise mixed valence states of iron (*i.e.*, Fe^{3+} and Fe^{4+}) and cobalt (Co^{2+} and Co^{3+}), respectively. Thus, the resulting H_2 might reduce the valence state of MOFs' metal sites which then reduced bromate to bromide as illustrated in Fig. 5(d) [10]. In Fig. S9(a) (see **ESI†**), we also found that the XPS spectra of the spent MIL-88A after the bromate reduction still consisted of mixed valence states of iron (*i.e.*, Fe^{4+} and Fe^{3+}) and peak intensities of each states varied slightly compared to the pristine MIL-88A. This suggests that the transformation of valence states of iron was involved during the bromate reduction. It was expected that a higher oxidation state was reduced by H_2 and the reduce form of metal then reacted with bromate to become bromide. A similar result was also observed for the spent ZIF-67 which also exhibited mixed valence states of cobalt (*i.e.*, Co^{2+} and Co^{3+}) (Fig. S9(b)). It can be also noted that peak intensity of Co^{2+} greatly increased compared to that of the pristine ZIF-67, showing that the higher oxidation state of cobalt (Co^{3+}) was reduced to Co^{2+} with the assistance of H_2.

Moreover, although bromate removed from water was almost completely converted to bromide using both MIL-88A and ZIF-67 with $NaBH_4$, the amount of bromate reduction achieved using MIL-88A/$NaBH_4$ was much less than

ZIF-67/$NaBH_4$. In fact, the q_e of MIL-88A/$NaBH_4$ was around a half of that of ZIF-67/$NaBH_4$. This is possibly because active sites of MIL-88A were less accessible as its surface area and pore volume were significantly lower than ZIF-67. Besides, iron content in MIL-88A is estimated to be 19 wt% [53], which is also much less compared to cobalt content in ZIF-67, 26 wt% [54]. Therefore, active catalytic sites in ZIF-67 were much more and more accessible, leading to the higher removal efficiency.

3.3 Effects of $NaBH_4$ dosage and MOF loading on the bromate reduction

As MIL-88A and ZIF-67 can facilitate the hydrolysis of $NaBH_4$ to reduce bromate, the availability of $NaBH_4$ appears to be an important factor. Thus, the effect of $NaBH_4$ dosage was particularly examined. Fig. 6(a) reveals that when $NaBH_4$ dosage was varied from 500 to 600 mg L^{-1}, the q_e of MIL-88A for bromate was considerably increased from 0.63 to 1.11 mmol g^{-1} (Table S1, see **ESI**†) As $NaBH_4$ dosage was further raised to 1000 mg L^{-1}, the q_e correspondingly increased to 1.56 mmol g^{-1} (*i.e.*, 200 mg g^{-1}), showing that bromate was completely removed from water. Additionally, we also observed that the kinetics of bromate removal was noticeably faster with a higher $NaBH_4$ dosage. This suggests that the increase in $NaBH_4$ dosage not only improved the removal efficiency but also enhanced the removal kinetics. To quantitatively evaluate the effect of $NaBH_4$ dosage on kinetics, the pseudo first order rate law was employed as follows (Eq.(3)):

$$q_t = q_e \times (1 - \exp(-k_1 \times t)) \qquad (3)$$

where q_t and q_e are the removal efficiencies at mixing time t and equilibrium, respectively. k_1 (min^{-1}) represents the pseudo first order rate constant. The rate constants of bromate reduction using MIL-88A/$NaBH_4$ are determined and

summarized in Table 1. It can be seen that a higher $NaBH_4$ dosage significantly increased the kinetics. Fig. 7(a) also shows the q_t of the resulting bromide during the bromate reduction using MIL-88A with different $NaBH_4$ dosages. The amount of bromate removal was completely converted to bromide and a higher $NaBH_4$ dosage also led to a higher amount of bromide.

On the other hand, the effect of $NaBH_4$ dosage on the bromate reduction using ZIF-67/$NaBH_4$ was also examined. Considering that ZIF-67 with 500 mg L^{-1} of $NaBH_4$ had already completely reduced bromate to bromide, lower $NaBH_4$ dosages were intentionally evaluated as shown in Fig. 6(b). When $NaBH_4$ was lowered to 400 mg L^{-1}, 100 mg L^{-1} (*i.e.*, 0.78 mmol L^{-1}) of bromate in water was still completely reduced. However, the corresponding kinetics was found to be noticeably slower than that with 500 mg L^{-1} of $NaBH_4$. As $NaBH_4$ dosage was further reduced to 200 mg L^{-1}, the kinetics was significantly decreased. We also estimated the corresponding rate constants by fitting the kinetic data using Eq. 3 and fitting results can be seen in Fig. S10. k_1 value (Table 1) was substantially lowered when $NaBH_4$ dosage was reduced. However, as observed in Fig. 6(b), the bromate in water was still fully removed in the end of the reaction, despite the fact that $NaBH_4$ dosage became much lower. This suggests that 200 mg L^{-1} of $NaBH_4$ dosage was sufficient to completely reduce 100 mg L^{-1} of bromate in water with 500 mg L^{-1} of ZIF-67. In contrast, when $NaBH_4$ dosage was raised to 1000 mg L^{-1}, bromate was removed completely within an even shorter time and k_1 value became much higher, confirming that an increase in $NaBH_4$ dosage significantly enhanced the kinetics. Fig. 7(b) also reveals q_t of the resulting bromide using ZIF-67 with different $NaBH_4$ dosages. Amounts of bromate removal from water had been also completely turned into bromide. Additionally, by comparing k_1 values obtained using MIL-88A and ZIF-67 with the same $NaBH_4$ dosage, the

reaction kinetics of MIL-88A/$NaBH_4$ seemed slightly faster than that of ZIF-67/$NaBH_4$. Since the structure of MIL-88A was quite flexible [37], its pores might be closed or restricted from reactants. As a result, its active sites were mainly present on its external surface, leading to a faster reaction rate. Nevertheless, ZIF-67 exhibited a large pore volume, indicating that a part of active sites were inside pores of ZIF-67 and reactants had to diffuse into the pores of ZIF-67. Thus, the reaction kinetics was slightly slower but the removal efficiency was much higher using ZIF-67 than using MIL-88A.

In this study, another important parameter, MOF loading, was also investigated. At first, MIL-88A loading was varied from 250 to 1000 mg L^{-1} while fixing $NaBH_4$ dosage to 500 mg L^{-1}. As MIL-88A loading was lowered from 500 to 250 mg L^{-1}, the total amount of bromate removal (mmol) still remained similar (Fig. S11). This indicates that the q_t obtained using 250 mg L^{-1} of MIL-88A became higher than that obtained using 500 mg L^{-1} of MIL-88A as seen in Fig. 8(a). When MIL-88A loading was raised to 1000 mg L^{-1}, the total amount of bromate removal was still comparable to that obtained using 500 mg L^{-1} of MIL-88A (Fig. S11). This counterintuitive result indicates that despite a higher loading of MIL-88A, the total amount of bromate removal was not greatly improved, leading to a relatively low q_t value as seen in Fig. 8(a). In comparison with the effect of $NaBH_4$, the effect of MIL-88A loading seemed to be insignificant.

The effect of ZIF-67 loading was also examined by varying ZIF-67 loading from 250 to 1000 mg L^{-1}. The total amount of bromate removal using different ZIF-67 loadings is displayed in Fig. S11. While a higher ZIF-67 loading appears to increase the reduction kinetics, the total amounts of bromate removal at equilibrium using

different loadings are also similar. Thus, a higher q_t can be obtained using a lower ZIF-67 loading as shown in Fig. 8(b).

Despite the fact that bromate removed from water had been completely reduced to bromide regardless of MOF loading (Fig. S12), the effect of MOF loading was found to be negligible.

3.4 Effects of temperature and pH on the bromate reduction

Next, we examined the effect of temperature on the bromate reduction by varying temperature from 25 to 75 °C. As shown in Fig. 9(a), an increase in temperature did not result in a higher q_t but the kinetics was found to be faster. To quantitatively determine the effect of temperature on the kinetics, the pseudo first order rate law was also employed to analyze the kinetics at different temperatures. Fitting curves using the pseudo first order equation (Eq. 3) are shown as solid lines in Fig. S13(a). It can been found that the kinetics data were well fitted by the solid lines and rate constants were estimated and listed in Table 1. Although the q_t remained almost the same, the rate constant was significantly improved from 0.53 to 2.96 min^{-1} as temperature increased from 25 to 75 °C. In the case of ZIF-67 (Fig. 9(b)), the improvement in the kinetics can be more easily recognized. The kinetics data at different temperatures were also well-fitted by the pseudo first order equation (Fig. S13(b)) and rate constants are summarized in Table 1. The k_1 value at 75 °C was almost 10 times the k_1 value obtained at 25 °C, revealing the critical effect of temperature on the bromate reduction. As temperature appears to be such an influential factor, the relationship between temperature and rate constant was further analyzed using the Arrhenius equation as follows (Eq.(4)):

$$\ln k_1 = \ln k - E_a/RT \quad (4)$$

where k is the temperature-independent factor (g mg^{-1} min^{-1}); E_a represents the activation energy of the bromate reduction (kJ mol^{-1}); R is the universal gas constant and T is the solution temperature in Kelvin (K). Fig. S14 (see **ESI**†) shows plots of $1/T$ versus ln k_1 for the bromate reduction using MIL-88A/$NaBH_4$ and ZIF-67/$NaBH_4$. The data points can be properly fitted using Eq. (4) with correlation coefficients > 0.95, suggesting that the relationship between temperature and rate constant can be described by the Arrhenius equation. The corresponding E_a and k values are also determined in Table 2. It can be seen that the E_a obtained using ZIF-67/$NaBH_4$ is much higher than that obtained using MIL-88A/$NaBH_4$. This indicates that the bromate reduction was less difficult to occur using MIL-88A/$NaBH_4$ compared to ZIF-67/$NaBH_4$. Nonetheless, ZIF-67/$NaBH_4$ exhibited a distinctly higher removal efficiency than MIL-88A/$NaBH_4$.

Furthermore, the effect of pH on the bromate reduction was studied as shown in Fig. 10. In the case of MIL-88A/$NaBH_4$, the q_e was found to remain quite stable in the range of pH = 6−11. When pH was decreased to 5 and even lower, the q_e slightly increased. At pH = 3, the q_e was almost two times the q_e obtained at pH = 7, suggesting that acidic conditions seemed to improve the bromate reduction. On the other hand, the effect of pH was also investigated on the bromate reduction using ZIF-67/$NaBH_4$. It can be noted that in the pH range of 3−5, the bromate present in water was completely removed while the q_e was decreased gradually when pH was increased to 6 and higher. This result agrees with the finding seen in the case of

MIL-88A/$NaBH_4$ and the acidic condition appears to be more favorable for the bromate reduction.

3.5 Effects of co-existing anions on the bromate reduction

Occurrence of bromate is attributed to ozonation of bromide-containing water which may also comprise other anions, such as nitrate, sulfate and phosphate. Thus, it is another important aspect to understand whether co-existing anions affect the bromate removal using MOFs/$NaBH_4$. To evaluate the effect of co-existing anions, bromate solution consisting of equal-molar concentrations of bromate, nitrate, sulfate and phosphate were prepared. Plots of q_t versus reaction time for MIL-88A/$NaBH_4$ and ZIF-67/$NaBH_4$ are shown in Fig. 11. Fig. 11(a) reveals that MIL-88A/$NaBH_4$ could still remove bromate from water while Fig. 12(a) indicates that the amount of bromate removal was also reduced to bromide. Compared to the q_t in the absence of the co-existing anions, the q_t obtained here was comparable, indicating that the presence of the co-existing did not hinder the reduction of bromate using this MOFs/$NaBH_4$ process. Nevertheless, it can be noted in Fig. 11(a) that a considerable amount of phosphate was removed from water while only a small amount of nitrate and none of sulfate were removed at the end of the reaction. Since MIL-88A contains a metal-oxide structure similar to iron oxide which has been found to adsorb phosphate in water [55], the phosphate removal could be owing to the adsorption to MIL-88A. As a small amount of nitrate was removed, we also found the appearance of nitrite in the end of the reaction, showing that the catalytic hydrogenation was also capable of reducing nitrate to nitrite. This can be a worth-investigating topic in the future.

In the case of ZIF-67, the q_t in the absence of the co-existing anions was comparable to that obtained in the presence of the anions. Fig. 12(b) also reveals that

the amount of bromate removal had been almost completely converted to bromide, suggesting that the co-existing anions did not interfere with the reduction process of ZIF-67/$NaBH_4$. Unlike MIL-88A, the phosphate removal by ZIF-67 was much less, although small amounts of phosphate, nitrate and sulfate were still noticed during the bromate reduction.

3.6 Removal of low-level bromate from water and recyclability of MOFs for the bromate reduction

The afore-mentioned results clearly indicate that MOFs/NaBH4 appeared to be an effective system to reduce bromate to bromide. Since the typical bromate concentration is a few hundreds μg L^{-1} [56], we particularly evaluated whether MOFs/NaBH4 system can effectively treat bromate-containing wastewater. Fig. S15 shows C_t/C_0 versus reaction time for 100 μg L^{-1} of bromate using MIL-88A and ZIF-67 with $NaBH_4$. Both MIL-88A and ZIF-67 with $NaBH_4$ completely reduced 100 μg L^{-1} of bromate within 20 min, showing that MOFs/$NaBH_4$ is efficient to treat bromate-contaminated water. It is also noted that the reduction kinetics of MIL-88A/$NaBH_4$ seemed to be faster than ZIF-67/$NaBH_4$, which agrees with the findings observed when C_t was much higher (*e.g.*, 100 mg L^{-1}).

Furthermore, MOFs were evaluated for their recyclability for the bromate reduction. To test the recyclability of MOFs, the spent MOFs were collected and directly used for subsequent cycles without any regeneration treatments. Fig. 13 shows the recyclability of MIL-88A/$NaBH_4$ over 5 cycles. Although a slight loss was observed after 5 cycles, the recyclability (q_e of the spent MOFs over q_e of the pristine MOFs) remained around 90%. In the case of ZIF-67, the recyclability over 5 cycles was almost unchanged. This result reveals that even though MIL-88A and ZIF-67 can

be re-used to reduce bromate in the presence of $NaBH_4$, ZIF-67 seemed to be a relatively stable catalyst for such a reaction. The spent MOFs were also recovered and analyzed using XRD as shown in Fig. S16. Although peak intensities of the spent MIL-88A were slightly changed, possibly owing to its flexible structure being altered, the pattern remained similar to that of the pristine MIL-88A. XRD pattern of the ZIF-67 was also found to be comparable to that of the pristine ZIF-67. We also investigated whether Fe and Co leached out from MIL-88A and ZIF-67, respectively, during the bromate reduction. However, no Fe or Co was found in the bromate solution, showing the great stability of MIL-88A and ZIF-67 during the bromate reduction.

4. Conclusion

In this study, MOFs, as the first attempt, were used to remove bromate from water in the presence of $NaBH_4$. The iron-bearing MOF, MIL-88A, and the cobalt-bearing MOF, ZIF-67, were particularly selected as representative MOFs owing to their non-noble metallic contents. While $NaBH_4$ alone was found to reduce bromate, the combination of MOFs/$NaBH_4$ accelerated the hydrolysis of $NaBH_4$, thereby reducing bromate to bromide via hydrogenation. Factors influencing the bromate reduction were investigated including $NaBH_4$ dosage, MOF loading, temperature, pH and co-existing anions. The effect of $NaBH_4$ dosage was found to be the most influential on the removal efficiency and kinetics, while the effect of MOF loading was insignificant. Elevated temperatures and relatively acidic conditions were also more favorable for the bromate reduction in terms of the kinetics and removal efficiency, respectively. When other anions were present in the bromate solution, MOFs/$NaBH_4$ still successfully reduced bromate to bromide and the removal efficiencies were

comparable to those in the absence of the other anions. The recyclability tests revealed that MOFs/$NaBH_4$ can be re-used and ZIF-67/$NaBH_4$ even exhibited almost 100% of recyclability after 5 cycles. Although both MIL-88A and ZIF-67 with $NaBH_4$ can reduce bromate to bromide, ZIF-67 appears to be a better selection for MOFs owing to its much higher surface area and pore volume, and higher active catalytic content. The above-mentioned results indicate that MOFs can successfully facilitate the hydrolysis of $NaBH_4$ and subsequently reduce bromate to bromide in water.

References:

1. U. Pinkernell and U. von Gunten, *Environ. Sci. Technol.*, 2001, 35, 2525-2531.
2. M. M. Huber, S. Canonica, G.-Y. Park and U. von Gunten, *Environmental Science & Technology*, 2003, 37, 1016-1024.
3. G. L. Amy, M. S. Siddiqui and A. R. Foundation, *Strategies to Control Bromate and Bromide*, AWWA Research Foundation and American Water Works Association, 1999.
4. R. Song, R. Minear, P. Westerhoff and G. Amy, *Environmental Technology*, 1996, 17, 861-868.
5. K. Listiarini, J. T. Tor, D. D. Sun and J. O. Leckie, *Journal of Membrane Science*, 2010, 365, 154-159.
6. A. Bhatnagar, Y. Choi, Y. Yoon, Y. Shin, B.-H. Jeon and J.-W. Kang, *J Hazard. Mater.*, 2009, 170, 134-140.
7. J. A. Wiśniewski and M. Kabsch-Korbutowicz, *Desalination*, 2010, 261, 197-201.
8. H. Chen, Z. Xu, H. Wan, J. Zheng, D. Yin and S. Zheng, *Applied Catalysis B: Environmental*, 2010, 96, 307-313.
9. Y. Marco, E. García-Bordejé, C. Franch, A. E. Palomares, T. Yuranova and L. Kiwi-Minsker, *Chem. Eng. J.*, 2013, 230, 605-611.
10. J. Restivo, O. S. G. P. Soares, J. J. M. Órfão and M. F. R. Pereira, *Chem. Eng. J.*, 2015, 263, 119-126.
11. W. Sun, Q. Li, S. Gao and J. K. Shang, *J. Mater. Chem. A*, 2013, 1, 9215-9224.
12. X. Wu, Q. Yang, D. Xu, Y. Zhong, K. Luo, X. Li, H. Chen and G. Zeng, *Industrial & Engineering Chemistry Research*, 2013, 52, 12574-12581.
13. T. E. Crozier and S. Yamamoto, *J. Chem. Eng. Data*, 1974, 19, 242-244.
14. S. Özkar and M. Zahmakıran, *Journal of Alloys and Compounds*, 2005, 404–406, 728-731.
15. Y. Kojima, K.-i. Suzuki, K. Fukumoto, M. Sasaki, T. Yamamoto, Y. Kawai and H. Hayashi, *International Journal of Hydrogen Energy*, 2002, 27, 1029-1034.
16. B. H. Liu and Z. P. Li, *Journal of Power Sources*, 2009, 187, 527-534.
17. W. Ye, H. Zhang, D. Xu, L. Ma and B. Yi, *Journal of Power Sources*, 2007, 164, 544-548.
18. D. Hua, Y. Hanxi, A. Xinping and C. Chuansin, *International Journal of Hydrogen Energy*, 2003, 28, 1095-1100.

19. G. Guella, C. Zanchetta, B. Patton and A. Miotello, *The Journal of Physical Chemistry B*, 2006, 110, 17024-17033.
20. Y. Lee, Y. Kim, H. Jeong and M. Kang, *Journal of Industrial and Engineering Chemistry*, 2008, 14, 655-660.
21. D. Xu, H. Zhang and W. Ye, *Catalysis Communications*, 2007, 8, 1767-1771.
22. H.-C. J. Zhou and S. Kitagawa, *Chem. Soc. Rev.*, 2014, 43, 5415-5418.
23. N. Stock and S. Biswas, *Chemical Reviews*, 2011, 112, 933-969.
24. J. Lee, O. K. Farha, J. Roberts, K. A. Scheidt, S. T. Nguyen and J. T. Hupp, *Chemical Society Reviews*, 2009, 38, 1450-1459.
25. A. Corma, H. García and F. X. Llabrés i Xamena, *Chemical Reviews*, 2010, 110, 4606-4655.
26. N. L. Rosi, J. Eckert, M. Eddaoudi, D. T. Vodak, J. Kim, M. O'Keeffe and O. M. Yaghi, *Science*, 2003, 300, 1127-1129.
27. J. W. Yoon, S. H. Jhung, Y. K. Hwang, S. M. Humphrey, P. T. Wood and J. S. Chang, *Advanced Materials*, 2007, 19, 1830-1834.
28. J.-R. Li, Y. Ma, M. C. McCarthy, J. Sculley, J. Yu, H.-K. Jeong, P. B. Balbuena and H.-C. Zhou, *Coordination Chemistry Reviews*, 2011, 255, 1791-1823.
29. S.-H. Huo and X.-P. Yan, *J. Mater. Chem.*, 2012, 22, 7449-7455.
30. J. Shao, Z. Wan, H. Liu, H. Zheng, T. Gao, M. Shen, Q. Qu and H. Zheng, *J. Mater. Chem. A*, 2014, 2, 12194-12200.
31. K.-Y. A. Lin, H. Yang, C. Petit and F.-K. Hsu, *Chemical Engineering Journal*, 2014, 249, 293-301.
32. D. J. Tranchemontagne, J. R. Hunt and O. M. Yaghi, *Tetrahedron*, 2008, 64, 8553-8557.
33. M. Alvaro, E. Carbonell, B. Ferrer, F. X. Llabrés i Xamena and H. Garcia, *Chemistry – A European Journal*, 2007, 13, 5106-5112.
34. L. Shen, S. Liang, W. Wu, R. Liang and L. Wu, *Dalton Transactions*, 2013, 42, 13649-13657.
35. Q. Li and H. Kim, *Fuel Processing Technology*, 2012, 100, 43-48.
36. P. Horcajada, T. Chalati, C. Serre, B. Gillet, C. Sebrie, T. Baati, J. F. Eubank, D. Heurtaux, P. Clayette, C. Kreuz, J.-S. Chang, Y. K. Hwang, V. Marsaud, P.-N. Bories, L. Cynober, S. Gil, G. Ferey, P. Couvreur and R. Gref, *Nat Mater*, 2010, 9, 172-178.
37. T. Chalati, P. Horcajada, R. Gref, P. Couvreur and C. Serre, *J. Mater. Chem.*, 2011, 21, 2220-2227.
38. W.-T. Xu, L. Ma, F. Ke, F.-M. Peng, G.-S. Xu, Y.-H. Shen, J.-F. Zhu, L.-G. Qiu and Y.-P. Yuan, *Dalton Transactions*, 2014, 43, 3792-3798.

39. C. Mellot-Draznieks, C. Serre, S. Surblé, N. Audebrand and G. Férey, *J. Am. Chem. Soc.*, 2005, 127, 16273-16278.
40. J. J. Najera, C. J. Percival and A. B. Horn, *Phys. Chem. Chem. Phys.*, 2009, 11, 9093-9103.
41. E. M. S. Maçôas, R. Fausto, J. Lundell, M. Pettersson, L. Khriachtchev and M. Räsänen, *The Journal of Physical Chemistry A*, 2001, 105, 3922-3933.
42. E. Y. Ionashiro, F. J. Caires, A. B. Siqueira, L. S. Lima and C. T. Carvalho, *J. Therm. Anal. Calorim.*, 2012, 108, 1183-1188.
43. H. Bao, X. Chen, J. Fang, Z. Jiang and W. Huang, *Catal Lett*, 2008, 125, 160-167.
44. N. A. Ramsahye, T. K. Trung, L. Scott, F. Nouar, T. Devic, P. Horcajada, E. Magnier, O. David, C. Serre and P. Trens, *Chemistry of Materials*, 2013, 25, 479-488.
45. J. Cravillon, C. A. Schroder, H. Bux, A. Rothkirch, J. Caro and M. Wiebcke, *CrystEngComm*, 2012, 14, 492-498.
46. A. F. Gross, E. Sherman and J. J. Vajo, *Dalton Trans.*, 2012, 41, 5458-5460.
47. M. He, J. Yao, Q. Liu, K. Wang, F. Chen and H. Wang, *Microporous Mesoporous Mater.*, 2014, 184, 55-60.
48. J. Yao, R. Chen, K. Wang and H. Wang, *Microporous Mesoporous Mater.*, 2013, 165, 200-204.
49. A. Schejn, L. Balan, V. Falk, L. Aranda, G. Medjahdi and R. Schneider, *CrystEngComm*, 2014, 16, 4493-4500.
50. M. Kang, M. W. Song and C. H. Lee, *Applied Catalysis A: General*, 2003, 251, 143-156.
51. J. Li, G. Lu, G. Wu, D. Mao, Y. Guo, Y. Wang and Y. Guo, *Catalysis Science & Technology*, 2014, 4, 1268-1275.
52. E.-X. Chen, H. Yang and J. Zhang, *Inorganic Chemistry*, 2014, 53, 5411-5413.
53. C. Serre, F. Millange, S. Surblé and G. Férey, *Angewandte Chemie International Edition*, 2004, 43, 6285-6289.
54. R. Banerjee, A. Phan, B. Wang, C. Knobler, H. Furukawa, M. O'Keeffe and O. M. Yaghi, *Science*, 2008, 319, 939-943.
55. S.-Y. Yoon, C.-G. Lee, J.-A. Park, J.-H. Kim, S.-B. Kim, S.-H. Lee and J.-W. Choi, *Chem. Eng. J.*, 2014, 236, 341-347.
56. C. T. Matos, S. Velizarov, M. A. M. Reis and J. G. Crespo, *Environ. Sci. Technol.*, 2008, 42, 7702-7708.

Table 1. Kinetic modeling parameters for the bromate reduction (100 mg L^{-1}, equivalent to 0.78 mmol L^{-1}) using MIL-88A (500 mg L^{-1}) and ZIF-67 (500 mg L^{-1}).

MOFs	Conditions		Pseudo-first-order	
	Temp. (°C)	$NaBH_4$ (mg L^{-1})	k_1 (min^{-1})	R_1^2
MIL-88A	25	1000	2.20	0.998
	25	600	0.56	0.980
	25	500	0.53	0.992
	40	500	0.93	0.991
	50	500	1.74	0.994
	60	500	2.15	0.999
	75	500	2.96	0.999
ZIF-67	25	1000	2.14	0.997
	25	400	0.06	0.996
	25	500	0.13	0.986
	40	500	0.26	0.990
	50	500	0.29	0.981
	60	500	0.70	0.998
	75	500	1.45	0.999

Table 2. Activation Energy of the bromate reduction using MIL-88A and ZIF-67 in the presence of $NaBH_4$

MOFs	E_a (kJ mol^{-1})	k (g $mmol^{-1}$ min^{-1})
MIL-88A	30.2	113
ZIF-67	41.5	2100

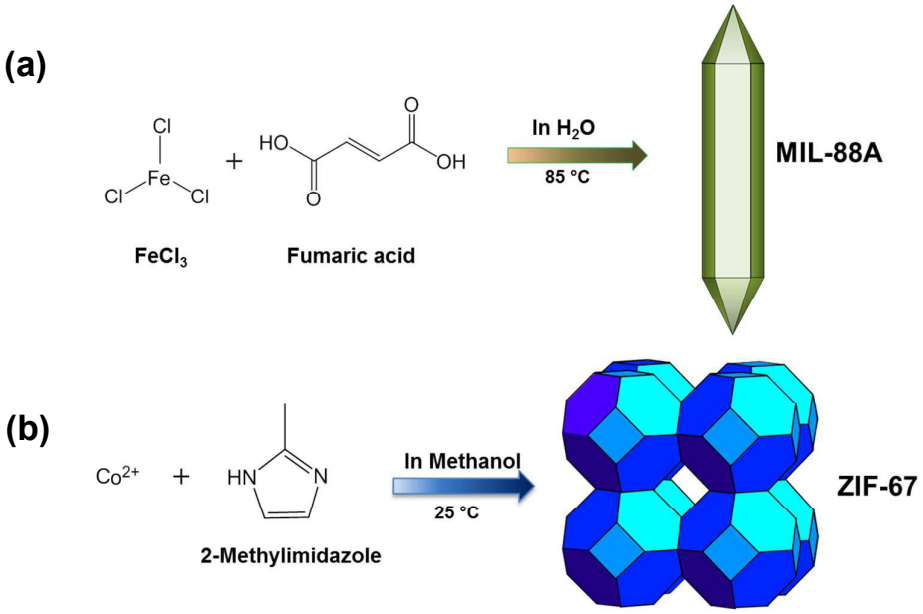

Fig. 1. Schematic illustration of syntheses of (a) MIL-88A and (b) ZIF-67

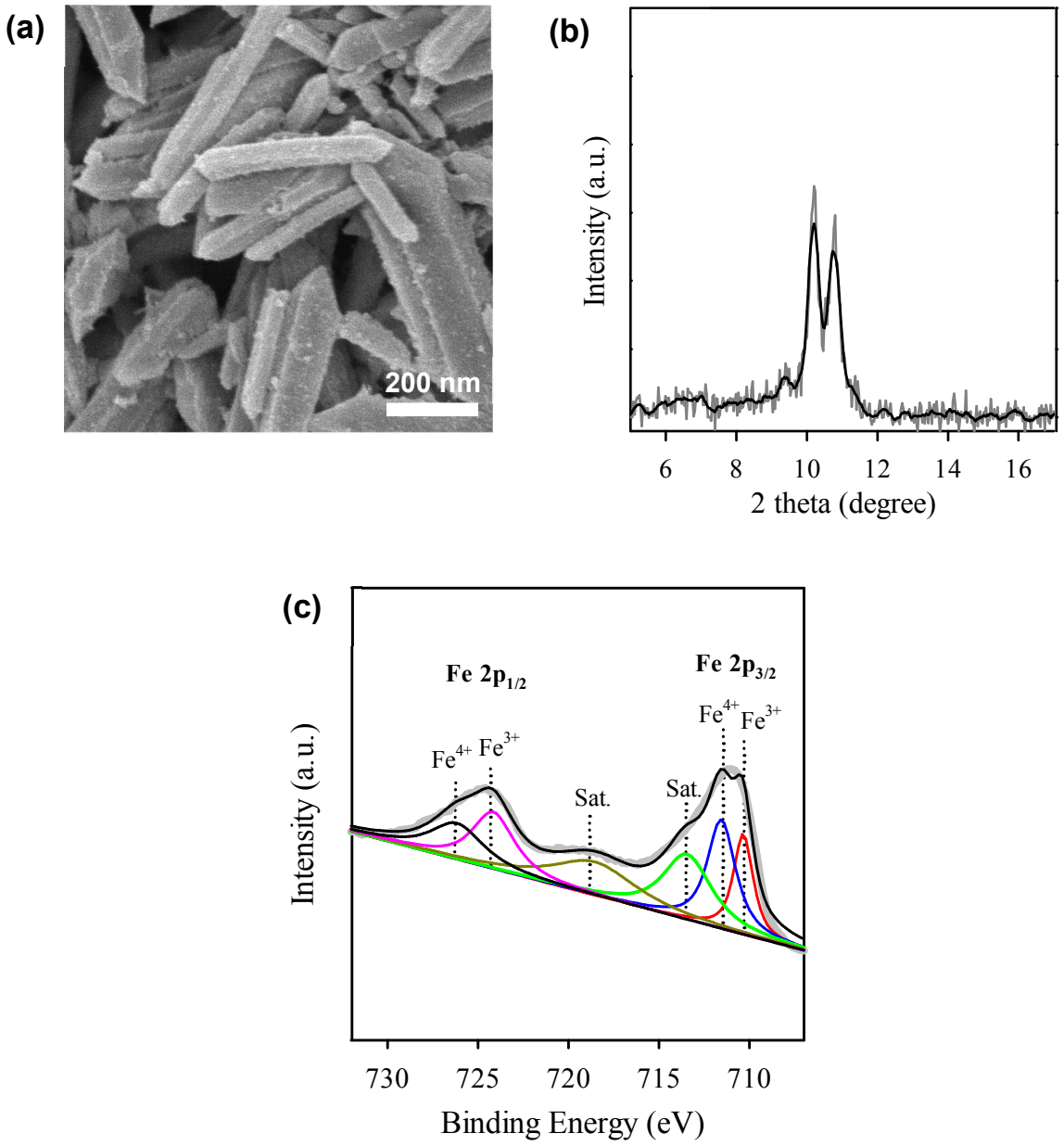

Fig. 2. Characterization of the as-synthesized MIL-88A: (a) SEM image, (b) XRD pattern and (c) Fe 2p core-level XPS spectrum of MIL-88A.

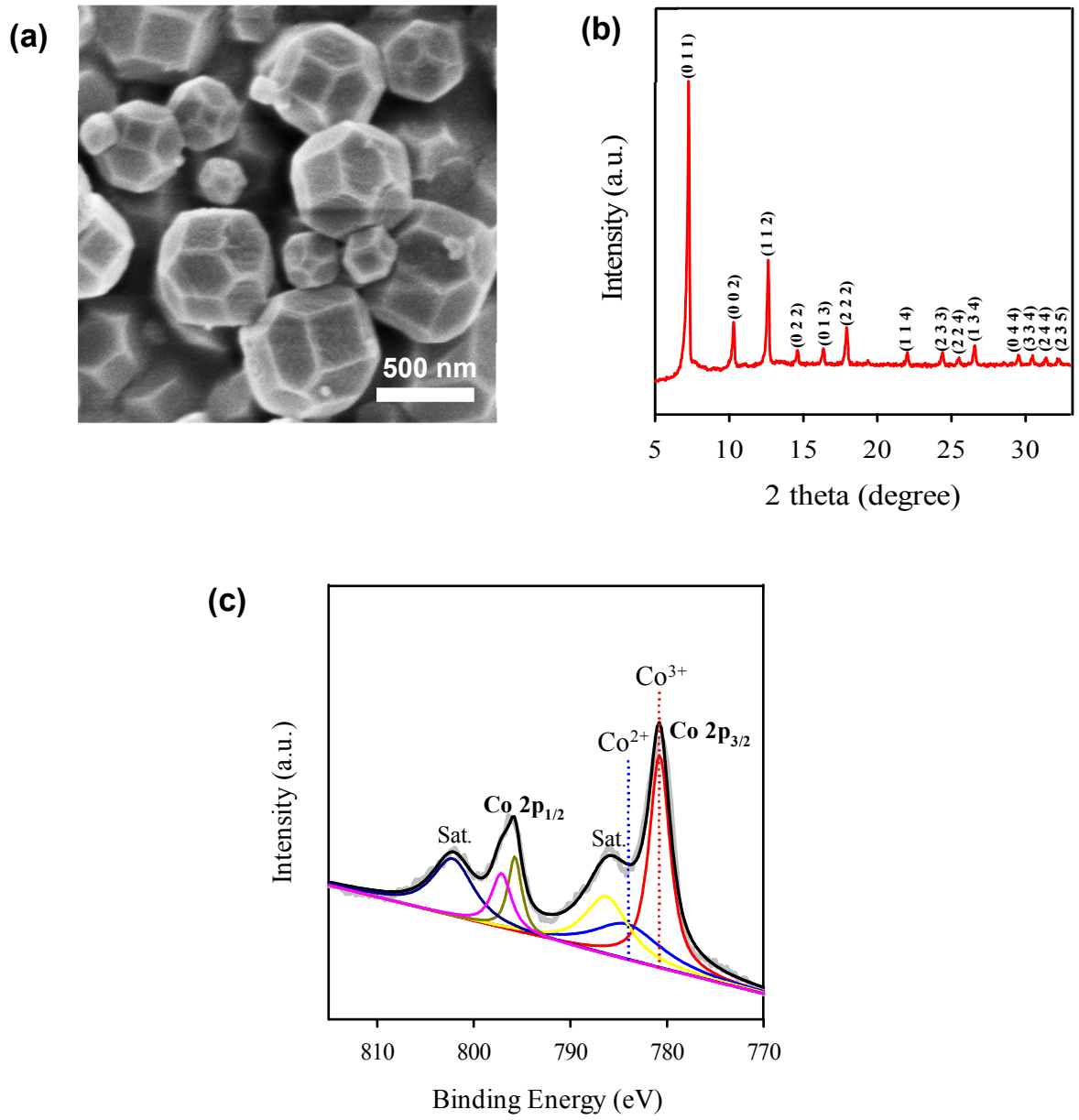

Fig. 3. Characterization of the as-synthesized ZIF-67: (a) SEM image, (b) XRD pattern and (c) Co 2p core-level XPS spectrum of ZIF-67.

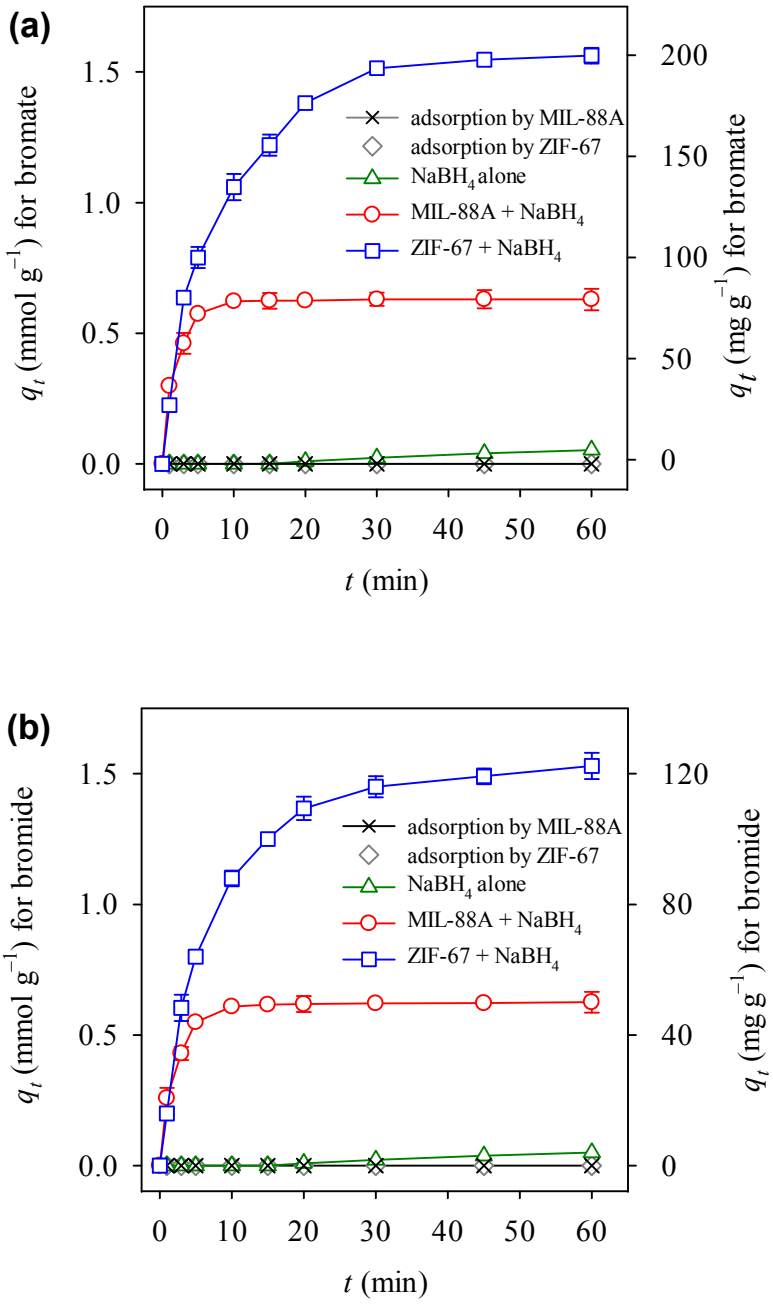

Fig. 4. Removal of bromate using (a) MIL-88A and ZIF-67 with and without $NaBH_4$, and (b) generation of bromide during the bromate removal (MOFs = 500 mg L^{-1}, $NaBH_4$ = 500 mg L^{-1}, T = 25 °C).

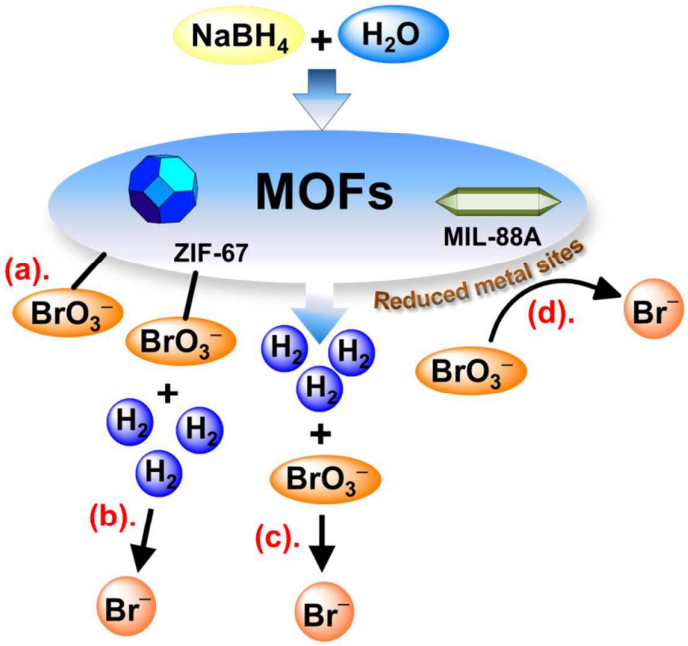

Fig. 5. Proposed mechanism for the bromate reduction using MOFs/$NaBH_4$: (a) bromate resides on the surface of MOFs, (b) H_2 generation from the hydrolysis of $NaBH_4$ facilitated by MOFs and H_2 reacted with bromate residing on the surface of MOFs to form bromide, (c) bromate in the bulk solution reacts with the resulting H_2 to form bromide, (d) reduced metal sites of MOFs induced by H_2 further reduces bromate to bromide.

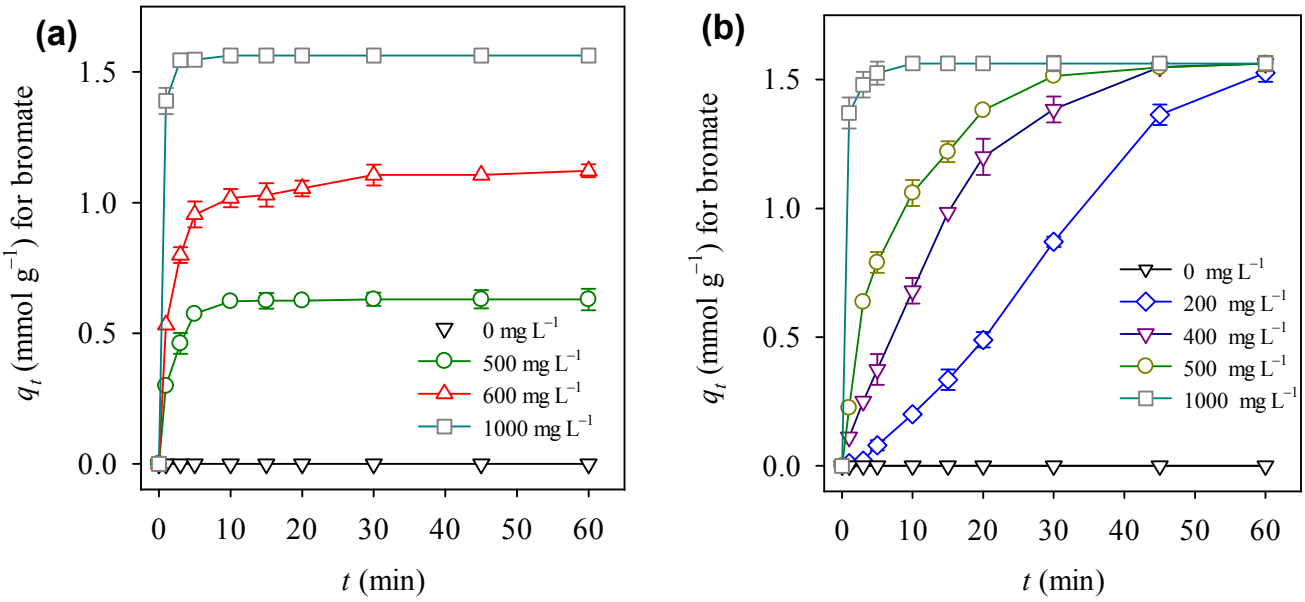

Fig. 6. Effect of $NaBH_4$ dosage on the bromate removal using (a) MIL-88A and (b) ZIF-67 (MOFs = 500 mg L^{-1}, T = 25 °C).

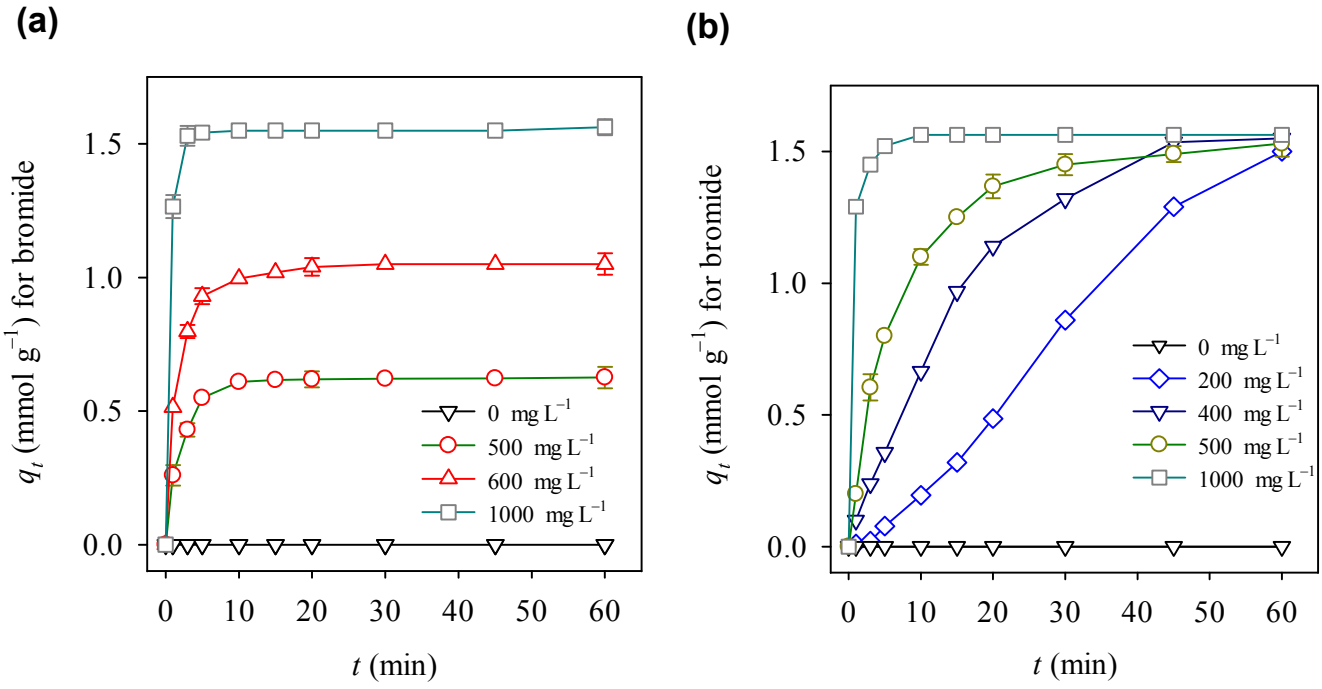

Fig. 7. Effect of $NaBH_4$ dosage on the generation of bromide using (a) MIL-88A and (b) ZIF-67 (MOFs = 500 mg L^{-1}, T = 25 °C).

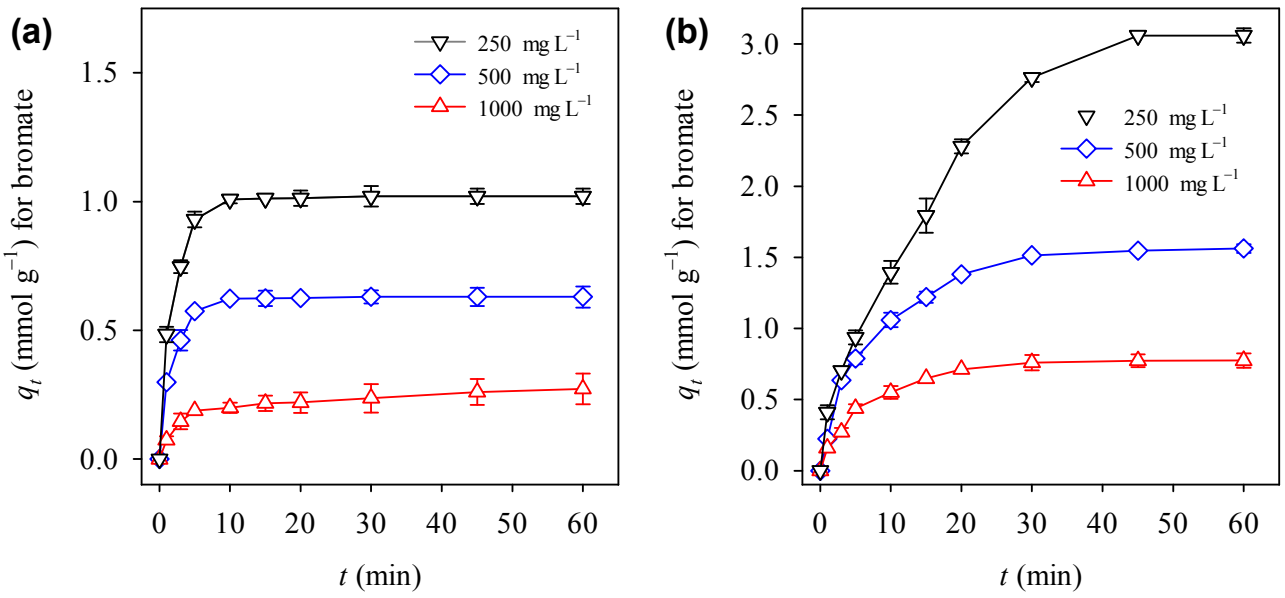

Fig. 8. Effects of (a) MIL-88A loading and (b) ZIF-67 loading on the reduction of bromate ($NaBH_4$ = 500 mg L^{-1}, T = 25 °C).

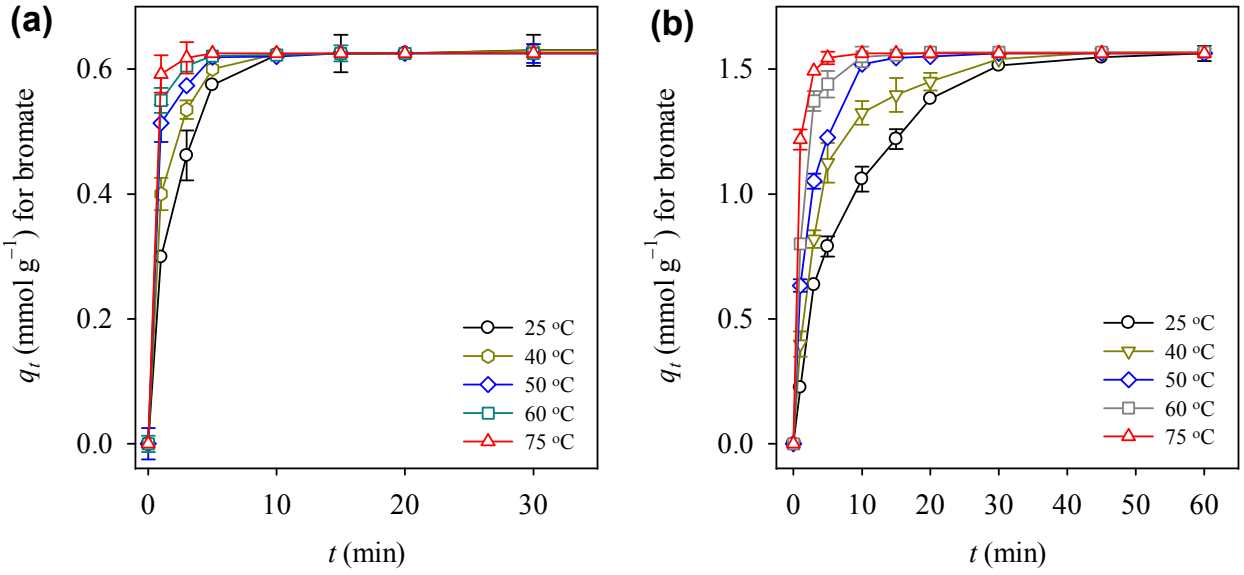

Fig. 9. Effect of temperature on the removal of bromate using (a) MIL-88A and (b) ZIF-67 (MOFs = 500 mg L^{-1}, $NaBH_4$ = 500 mg L^{-1}).

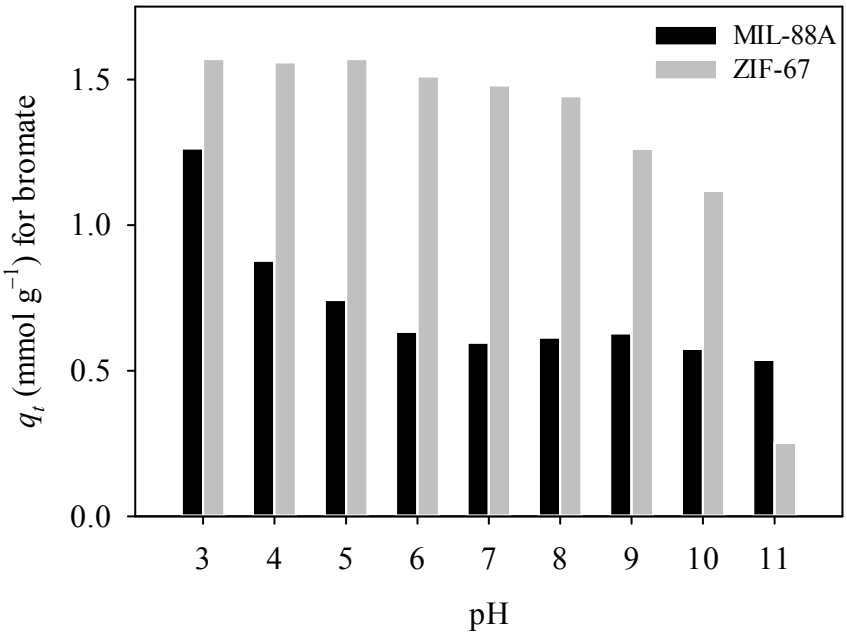

Fig. 10. Effect of pH on the removal of bromate using MIL-88A and ZIF-67 with $NaBH_4$ (MOFs = 500 mg L^{-1}, $NaBH_4$ = 500 mg L^{-1}, T = 25 °C).

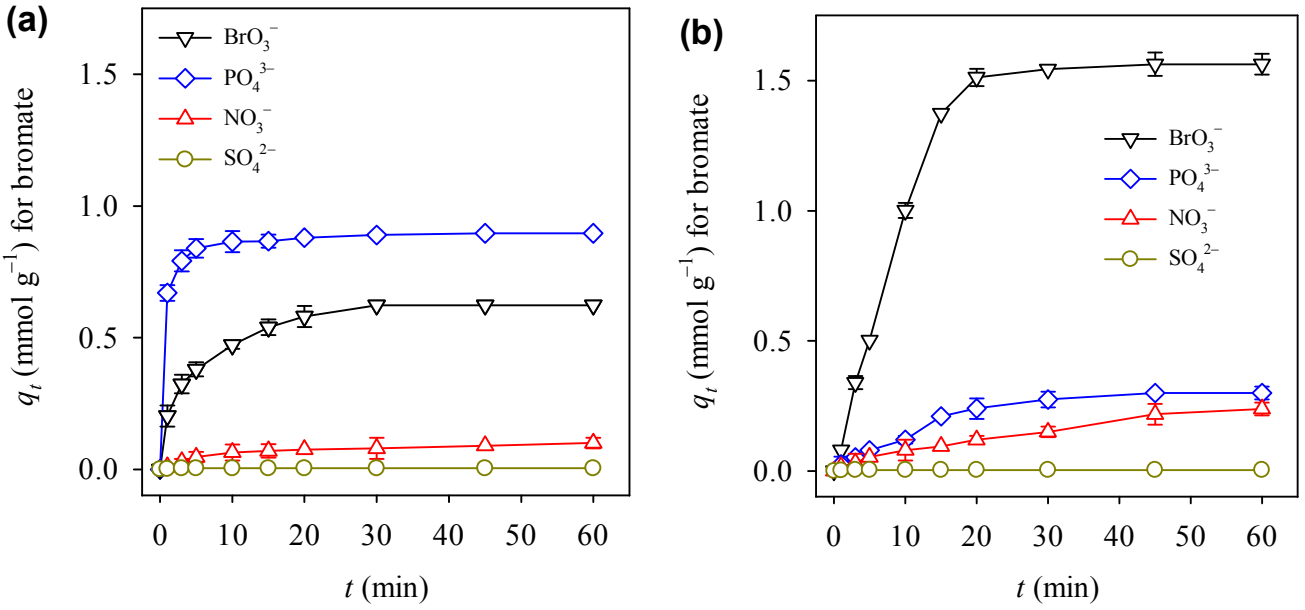

Fig. 11. Effect of co-existing ions on the reduction of bromate using (a) MIL-88A and (b) ZIF-67 (MOFs = 500 mg L^{-1}, $NaBH_4$ = 500 mg L^{-1}, T = 25 °C).

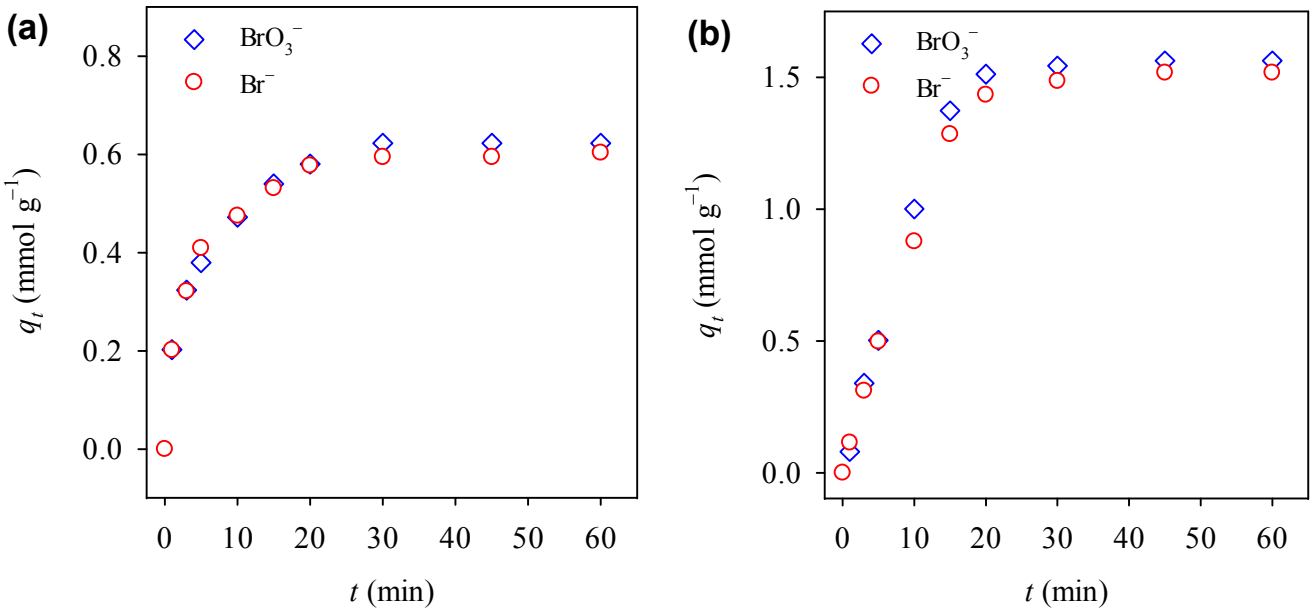

Fig. 12. Reduction of bromate to bromide in the presence of co-existing ions using (a) MIL-88A and (b) ZIF-67 (MOFs = 500 mg L^{-1}, $NaBH_4$ = 500 mg L^{-1}, T = 25 °C).

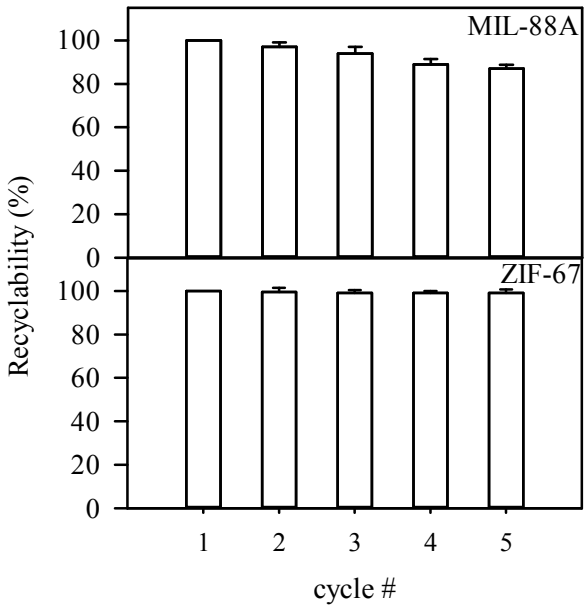

Fig. 13. Recyclability of MIL-88A and ZIF-67 for the reduction of bromate to bromide (MOFs = 500 mg L^{-1}, $NaBH_4$ = 500 mg L^{-1}, T = 25 °C).